Available online at www.sciencedirect.com

ScienceDirect

Energy Procedia 126 (201709) 219–226

Energy Procedia

www.elsevier.com/locate/procedia

72nd Conference of the Italian Thermal Machines Engineering Association, ATI2017, 6-8 September 2017, Lecce, Italy

Comparing energy performance of different semi-transparent, building-integrated photovoltaic cells applied to "reference" buildings

Francesco Martellotta*, Alessandro Cannavale, Ubaldo Ayr

Dipartimento di Scienze dell'Ingegneria Civile e dell'Architettura – Politecnico di Bari, via Orabona 4, 70125 Bari (Italy)

Abstract

Semi-transparent, building-integrated photovoltaics (BIPVs) are receiving significant attention by several research groups, given their increasing efficiencies combined to improved visual performance (being cell transparency and color rendering index, two key features to ensure their widespread use). Several technologies have been developed in the last years, based on the use of amorphous silicon cells, Cu(In,Ga)Se2 (CIGS) cells, organic PV cells, photoelectrochemical (DSC) cells, and perovskite-based cells. Each technology has pros and cons, but among them the two most reliable and promising seem to be the first one (η_{STC}= 3-6% and T_{vis}= 7-40%) and the last one (η_{STC}= 6.6% and T_{vis}= 42.4%). The second, in particular, may be processed so to appear neutrally colored, resulting in a substantially gray glass, while the first one, absorbing nearly all the blue-green radiation, presents an orange-brown coloration. The paper investigates how the use of both technologies affects the energy balance of buildings. For this purpose the EnergyPlus platform was employed and two validated reference buildings were used for comparison (one residential and one office building). Energy yield due to BIPV technologies, variation in heating and cooling loads due to cell transparency, and implications on visual comfort and on artificial lighting usage are finally discussed

Peer-review under responsibility of the scientific committee of the 72nd Conference of the Italian Thermal Machines Engineering Association

Keywords: Building-integrated photovoltaics; energy performance; energy simulation.

* Corresponding author. Tel.: +39-080-5963631
E-mail address: francesco.martellotta@poliba.it

Peer-review under responsibility of the scientific committee of the 72nd Conference of the Italian Thermal Machines Engineering Association
10.1016/j.egypro.2017.08.143

1. Introduction

Building integrated photovoltaics (BIPV) represent nowadays one of the most impressive opportunities in favour of a widespread use of energy producing devices. In fact, integration of PV elements in building components represents a major advantage compared to conventional building applied PV (BAPV) systems, where PV panels are simply attached on exterior parts of building envelopes (on rooftops or facades). Consequently, as BIPV systems represent architecturally relevant components, they require the complex fulfillment of multiple conditions (aesthetic, economic, structural, acoustic, thermal, etc.) [1]. Façade elements, and transparent components in particular, are among the most interesting parts of the building that can conveniently integrate PV technologies. They cover large unobstructed surfaces (particularly for high rise buildings), have several exposures (allowing to follow sun path), may easily integrate wiring and other systems. Thus, several researchers are now investigating the potential of this technology, with particular reference to semi-transparent devices. [2]

Amorphous silicon solar cells (a-Si) [3] have currently reached the best laboratory efficiency of 10.2% [4]. This technology takes advantage of a much lower consumption of silicon with respect to first generation PVs, a lighter substrate (glass), a consolidated industrial process, and, above all, its range of applications is widened by its semitransparency. Several low-cost, lightweight and flexible a-Si:H semitransparent solar cells have already been reported in the literature [5].

Among the other technologies, semitransparent PV glazing based on 1.2 μm thick CIGS solar cells were reported, with a conversion efficiency of 5.6%. [6], organic PVs, currently offering 11.5% efficiency, are investigated for use in semi-transparent devices although durability concerns are currently hampering its use [7]. Photoelectrochemical cells, also known as dye sensitized cells (DSCs) have been long considered as a promising technology for semitransparent PV devices. However, several concerns limit their reliability.

More recently, perovskite-based solar cells have been revolutionizing the field because they are easily-processable, offer high conversion efficiency (up to 22%). Several strategies have been proposed in order to realize highly transparent perovskite cells. Among the most successful, making thinner perovskite layers leads to obtain brownish cells [8,9], while controlling the perovskite morphology, as to fabricate discontinuous micro-islands by tuning the physical parameters of the perovskite deposition process [10] leads to neutral-tinted films, with minimal impacts on the spectral properties of light entering indoor.

When dealing with transparent components, energy saving concerns suggest limiting cooling loads in buildings by means of solar control glasses. On the other hand, visual comfort considerations suggest minimum acceptable values for glazing transmittance, to range between 25% and 38% [11]. Thus, integration of semi-transparent devices which simultaneously limit solar gains and produce electric energy may become an interesting opportunity.

More recently, Chae et al. [12] suggested a procedure to evaluate the energy performance of buildings incorporating BIPVs, considering not only the electrical characteristics of PV cells, but also thermal and optical behavior and the consequent implications on building energy performance. They found that the maximum electric energy generation using a-Si:H cells could range from 22 kWh/m^2 per year to 45 kWh/m^2 per year, depending on several parameters including the type of PV cell, the site location and the exposition. Oliver et al. [13] studied the influence of building integrated semitransparent solar cells on heating, cooling and lighting loads and electricity generation, considering parameters like window-to-wall-ratio (WWR) and cells average visible transmittance (T_{vis}). They found out a promising energy saving potential between 18% (WWR=33%) and 59% (WWR=88%), compared to regular glass.

Following similar researches [12,14], this study aims at comparing the energetic advantages resulting from use of more consolidated a-Si technologies with those resulting from perovskite-based cells. The a-Si cells are the only semi-transparent PV technology already available on market. Among the best performing cells, those used by Chae et al. (η_{STC}=5.30%, T_{vis}=0.41) [12] and by Lim et al. (η_{STC}=5.93%, T_{vis}=0.18) [15] are worth being mentioned. On the other side, the best perovskite based semi-transparent cells achieved an efficiency of 6.4% while keeping high visible transmittance (0.424) [16]. Results of the comparisons are shown below.

2. Methods

2.1. PV cells

As an example of a-Si cells, those fabricated by Chae et al. [12] were considered. Among the three types of semi-transparent solar cells discussed in their paper, that with the highest transparency was considered, a textured solar cell with a 120-nm a-Si:H absorber. The front electrode was formed by depositing 1.5-µm-thick aluminium-doped zinc oxide (ZnO:Al) on a borofloat glass substrate (3 mm) in a sputtering chamber. The p–i–n a-Si:H solar cell stacks were deposited on a ZnO:Al/glass substrate via plasma-enhanced chemical vapour deposition at 250 °C. The thickness of the doped n-type and p-type a-Si:H films were both 10 nm and that of intrinsic absorber a-Si:H was 120 nm.

The neutral coloured semi-transparent perovskite solar cell devices used in this study were prepared according to the method described in Refs. [16,17]. The procedure involved the rigorous cleaning and patterning of FTO/glass substrates, the subsequent coating of a compact TiO_2 n-type layer and the deposition of dewetted perovskite islands. Shunt-blocking layers from Octadecyl-trichloro silane were additionally applied to improve the device performance before the hole transporting layer spiro-OMeTAD was deposited. A flexible nickel micro grid was laminated to act as a transparent hole conducting electrode.

A summary of the electric and optic characteristics of the selected cells are given in Table 1. In optical terms, as anticipated, a-Si cells absorb most of the blue-green radiation, so that they appear as brown-orange. Conversely, perovskite cells are neutrally colored, thus being mostly grayish (Fig. 1). Besides the parameters listed in the table, the two technologies differ in the dependence between conversion efficiency and radiation intensity. In fact, while for a-Si decreases mildly as intensity becomes lower than 1000 W/m^2, and then suddenly drops when radiation approaches zero [18], perovskite cells show a substantially linear behavior [17].

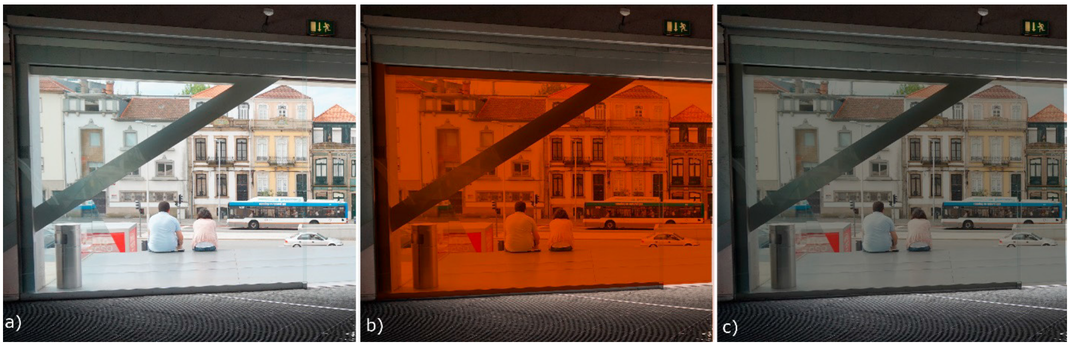

Fig. 1. Simulation of the appearance of the different technologies applied to a glazing. a) Baseline condition; b) a-Si cell; c) perovskite cell.

Table 1. Photovoltaic and optical parameters of solar cells used in the paper.

Cell type	Short-circuit current density (j_{sc}) [mA/cm^2]	Fill factor (FF)	Open circuit voltage (Voc) [V]	Conversion efficiency (η_{STC}) [%]	Visible transmittance (T_{vis}) [%]
a-Si:H	7.70	0.69	0.9030	4.80	30.1
Perovskite	11.03	0.65	0.9532	6.64	42.4

2.2. Building model description

The building models used in this study were taken from the archive of the reference buildings available from the US Department of Energy [19]. Such models differ, depending on the climatic conditions of the city they refer to.

So, for the purpose of the subsequent analysis, models referred to the city of Los Angeles were chosen, as its Koppen-Geiger classification is Csa (warm Mediterranean), the same of most Southern Italy cities. The first reference building is a medium-sized office building that has three floors and five thermal zones consisting of one core area and four external spaces (one for each exposure) in each floor (Fig. 2a). Total conditioned floor area is 10,000 m^2, approximately. The wall window ratio (WWR) is 30% and the total window area is 652 m^2. Envelope thermal resistance is 0.46 m^2K/W for ground floor, 2.74 m^2K/W for roof, and 1.42 m^2K/W for walls. The second reference building is a mid-rise apartment building, with four floors, 31 apartments and one office (Fig. 2b). The wall window ratio is 15%. Envelope thermal resistance is 0.46 m^2K/W for ground floor, 2.74 m^2K/W for roof, and 2.09 m^2K/W for walls. Daily internal load condition and pattern fraction of occupants, lighting, and equipment were left unchanged according to the "reference building" specifications, with 10.76 W/m^2 for both lighting and equipment loads in the office building and an occupancy rate of 18.58 m^2/person. In the apartment buildings lighting and equipment loads were respectively 3.88 W/m^2 and 5.38 W/m^2, with 2.5 persons per apartment.

Fenestration was assumed to have thermal–optical properties of a simple double-pane glazing system (3mm-clear glass/16mm-air gap/3mm-clear glass) as a baseline model. Clear glass was a Pilkington Optifloat Clear, with T_{vis} = 0.907. PV devices were applied only on South, East, and West windows and were assumed to be located on the inside face of the outside glass, they consequently affected both solar heat gain coefficient and the overall visual transmittance given by the product of the T_{vis} pertaining to the different layers. Variations in surface emissivity might slightly change the overall heat transfer coefficient (U-value), but such differences were negligible in the present case and the same value of 2.725 W/m^2K was used for the three glazings (Table 2).

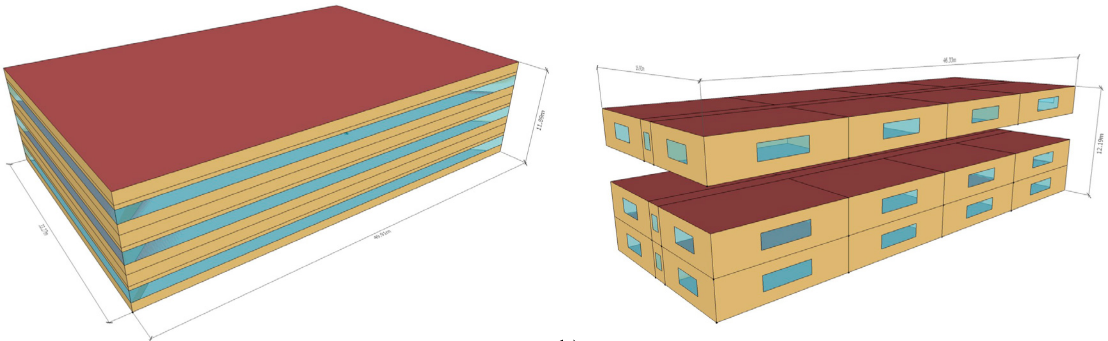

a) b)

Fig. 2. 3D model of the reference buildings: a) Medium office; b) Mid-rise apartment building.

Table 2. Glazing features as modelled.

Window type	Base-line	a-Si	Perovskite
SHGC	0.804	0.398	0.491
T_{vis}	0.828	0.274	0.388

All the analyses were carried out using EnergyPlus v. 8.6. In order to determine the heating and cooling energy consumptions in a simple and straightforward way, and also to avoid making assumptions on more detailed plant characteristics, an "IdealLoadAirSystem" with no outdoor air was considered. This EnergyPlus object provides both the heating and cooling energy required to meet the temperature set-points that have been provided by the relevant schedules. As the purpose of the analysis was that of determining the influence on energy consumptions for heating and cooling due to different glazing types, no restrictions were applied to the maximum sensitive heating capacity. As the IdealLoadAirSystem returns exactly the thermal energy that must be provided, to convert such value into electrical energy, a constant COP of 3 was assumed for both heating and cooling modes. In the office building, heating was turned on during working hours and off during nights and holydays. In the residential building systems were always turned on. In both cases, heating was turned on only during the period allowed by Italian regulations, while cooling was turned on from June 1st to September 30th.

With reference to the weather conditions, data taken from a large and homogeneous dataset were preferred. Consequently, the IWEC2 (International Weather for Energy Calculations) database developed by ASHRAE within the Research Project RP-1477, "Development of 3012 Typical Year Weather Files for International Locations" [20]. was preferred among others. All the analyses were carried out using the climate data for Bari/Palese Macchie.

Finally, in order to calculate energy yield due to BIPV cells, the equivalent one-diode model was used for a-Si employing electric data given in Table 1. For perovskite cells, as the relationship between efficiency and solar radiation is linear and cannot be accounted by any of the embedded EnergyPlus models, the following procedure was used. For each window the overall incident solar radiation rate per unit area was obtained for each timestep (every hour). Considering the linear relationship between efficiency and radiation intensity, the corresponding PV cell efficiency was first calculated at the reference temperature of 25 °C. Then, the outside surface temperature was obtained for each window (assuming that, due to reduced thickness and high thermal conductivity, the outside surface temperature corresponded to the PV cell temperature). The cell efficiency was consequently corrected to take into account the temperature effect, decreasing η by 0.3% every Celsius degree in excess of STC [17].

3. Results

3.1. Photovoltaic energy yield

As the energy yield per unit area depends only on the façade exposition and is independent on the type of building, it can be discussed first, so that the effects on the overall energy balance of the two case studies can be analyzed in more detail later. First of all, it can be observed that, as expected, the plot of efficiency as a function of sun irradiation (Fig. 3) shows that a-Si cells, despite the lower STC value, performed better than perovskite cells under low-radiation conditions. When averaged over an entire year, and referred to the different exposures, it clearly appears that a-Si cells outperform perovskite cells by a minimum of 30% on the South façade, up to a maximum of 180% on the North façade, confirming that the first technology is capable of taking advantage of diffuse radiation much better than the second. On the South façade, where the maximum energy yield is achieved, a-Si cells may provide up to 45 kWh/m^{2}year, while perovskite cells may provide up to 34.4 kWh/m^{2}year. East and west facades show mostly similar results, with a-Si yielding about 30 kWh/m^{2}year, and perovskite yielding about 21 kWh/m^{2}year. The strong dependence of solar radiation on the angle formed between the sun and the normal to the surface also suggests that, as demonstrated in Ref. [17], significant variations may be observed when changing the location.

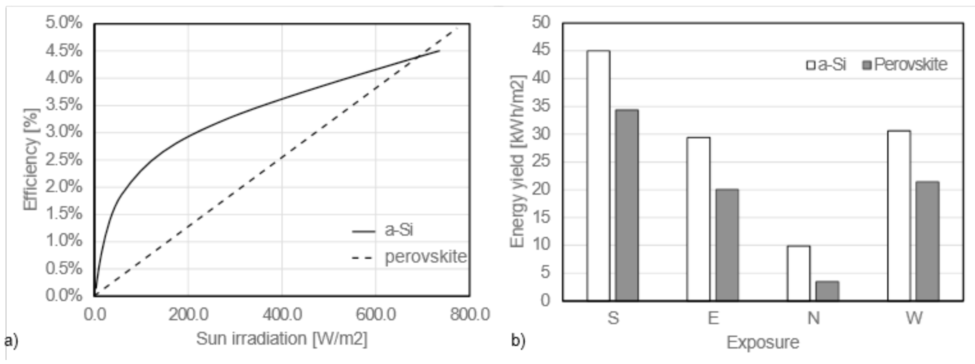

Fig. 3. Comparison of the PV energy yield obtained using a-Si:H and perovskite cells. a) Efficiency as a function of sun irradiation; b) Yearly energy yield per unit area as a function of exposure.

3.2. Energy balance of the “Medium Office”

With reference to the “Medium Office” results showed that, due to the large internal gains there was a significant imbalance between heating and cooling loads. They were translated into electricity consumption assuming a constant COP for both heating and cooling and the resulting values are given in Table 3. Compared to the Baseline case, using PV glazings determined a reduction of solar gains, so that heating consumptions increased slightly (by 2 MWh/year and 1.5 MWh/year for a-Si and perovskite cells respectively). However, the reduction in cooling consumptions was much bigger (being respectively 13.1 MWh/year and 9.8 MWh/year for a-Si and perovskite cells). Combining both heating and cooling yields an overall 83.5 MWh/year for the baseline conditions, followed by a 75.3 MWh/year for perovskite cells, and by a 72.4 MWh/year for a-Si cells. So, apparently, use of semi-transparent glazings had positive effects on the energy balance, even neglecting PV production. However, one possible side effect of using such glazing is related to a possible increase in electric consumption due to lighting. To take into account the contribution of daylighting, for each zone located along the perimeter the electric lighting was dimmed so that a minimum value of illuminance equal to 500 lx was kept at a reference point. The core zone was not included as it clearly cannot benefit of daylighting. Results showed that, as expected, the darker a-Si glazings caused an increase by 3.4 MWh/year compared to the baseline condition (clear glass), while perovskite cells caused an increase by 1.6 MWh/year. Finally, when the PV yield is taken into account the resulting balance shows that with reference to HVAC consumptions using BIPV solutions determined an impressive saving of 33.3% using a-Si and of 24.5% using perovskite cells. Lighting, with the large invariant contribution of the core zones, caused a reduction of the percent variation to 12.3% in the first case, and to 9.5% in the second. If the equipment consumptions (independent of the particular glazing used, and being about 1.5 times the other consumptions) were included in the analysis the variations would seem almost negligible. However, in absolute terms, it is possible to save between 20 and 28 MWh/year, resulting in a reduction in bills varying from 4000 to 5600 €.

Table 3. Summary of energy balance for the "Medium Office" building.

	Heating	Cooling	Lighting	Equip.	PV Yield	HVAC Balance	Var.	HVAC+Light Balance	Var.	Overall Balance	Var.
	[MWh/year]	[MWh/year]	[MWh/year]	[MWh/year]	[MWh/year]	[MWh/year]	[%]	[MWh/year]	[%]	[MWh/year]	[%]
Reference	5.1	78.4	115.1	295.8		83.5		198.7		494.5	
a-Si	7.1	65.3	118.5	295.8	16.65	55.8	-33.3%	174.3	-12.3%	470.1	-4.9%
Perovskite	6.6	68.7	116.7	295.8	12.15	63.1	-24.5%	179.8	-9.5%	475.6	-3.8%

In order to analyze in greater details the effects of the semi-transparent glazings on visual comfort, Useful Daylight Illuminance (UDI) parameter [21] was used to analyze light distribution inside the space throughout the year. The parameter is defined as the percentages of time in which illuminance due to daylight falls within an ideal range spanning between 300 lx and 3000 lx. Values below 300 lx are generally considered insufficient, and require a supplement of artificial light. Conversely, values above 3000 lx are likely to produce visual discomfort due to glare. As shown in Table 4, the baseline condition causes a lot of over-illumination, particularly on the south exposition. Conversely, a-Si glazing causes the highest percentage of under-illumination. Perovskite cells showed a more balanced behavior, returning the highest UDI across all the expositions.

Table 4. Summary of results of Useful Daylight Illuminance analysis for the "Medium Office" building.

	$UDI_{<300}$				$UDI_{300-3000}$				$UDI_{>3000}$			
	South	East	West	North	South	East	West	North	South	East	West	North
Reference	9%	9%	9%	10%	40%	60%	58%	90%	51%	30%	33%	0%
a-Si	23%	24%	24%	10%	77%	67%	64%	90%	0%	8%	12%	0%
Perovskite	16%	18%	18%	10%	77%	71%	68%	90%	7%	11%	15%	0%

3.3. *Energy balance of the* "*Mid-rise apartment building*"

Results for the "Mid-rise apartment" showed (Table 5) a significantly different picture compared to the office building. Differences in internal loads and in schedule of both heating and cooling systems caused the respective consumptions to be more similar. In fact, in the office cooling energy was 9 to 15 times higher than heating energy, while in the apartment building they vary between 2 and 2.75. Normalization referred to the overall floor surface area shows (Fig. 4) a much bigger difference in heating consumptions for the apartment building, while cooling energy requirements are mostly similar (as lower internal and external loads balanced the longer operation time). Lighting and equipment requirements are clearly lower than office, but they remain quite high for typical Italian households. In fact, they sum to 55 kWh/m^{2}year, meaning that a 100 m^2 house would require 5500 kWh/year, about twice the consumption estimated by Italian Energy Authority for typical families (2700 kWh/year). In the light of the above results, it is worth combining PV output only with HVAC consumptions in order to assess the residential building performance. The reduced WWR obviously affected the overall energy yield to 5.45 and 4.02 MWh/year, respectively for a-Si and perovskite cells. In relative terms, PV production is almost halved in agreement with the actual window surface per surface area. The percent variation referred to HVAC consumptions is –12.8% for a-Si cells and –9.5% for perovskite cells, and including lighting and equipment further decreases such values. In agreement with previous results a-Si cells performed 30% better than perovskite cells. Considering the more complex nature of residential buildings, the dependence of lighting consumptions on daylighting was not analyzed in this case.

Table 5. Summary of energy balance for the "Mid-rise apartment" building.

	Heating	Cooling	Lighting	Equip.	PV Yield	HVAC Balance	Var.	HVAC+Light Balance	Var.	Overall Balance	Var.
	[MWh/year]	[MWh/year]	[MWh/year]	[MWh/year]	[MWh/year]	[MWh/year]	[%]	[MWh/year]	[%]	[MWh/year]	[%]
Reference	17.8	49.0	48.2	124.5		66.8		115.0		239.5	
a-Si	21.0	42.7	48.2	124.5	5.45	58.3	-12.8%	106.5	-7.4%	231.0	-3.6%
Perovskite	20.1	44.3	48.2	124.5	4.02	60.5	-9.5%	108.7	-5.5%	233.2	-2.7%

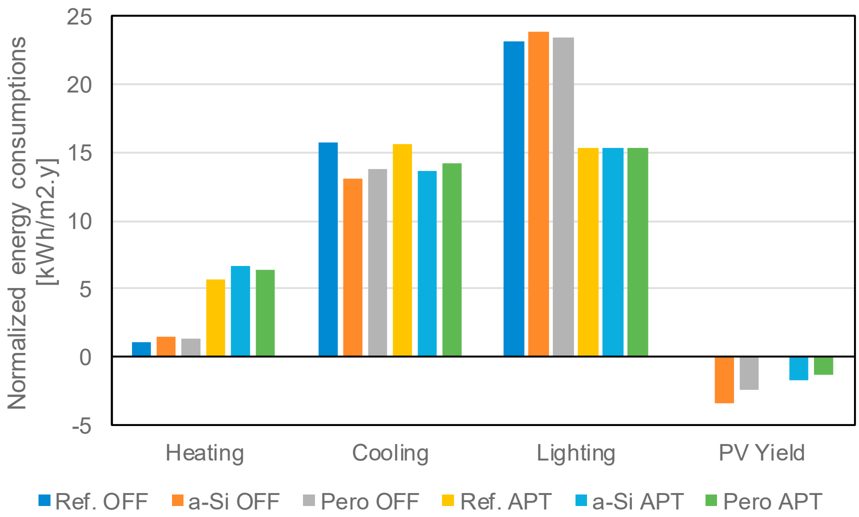

Fig. 4. Plot of energy consumptions due to heating, cooling, and lighting and PV production for office building (OFF) and apartment building (APT), normalized with reference to overall floor area.

4. Conclusions

The analysis pointed out that using BIPV technologies, with particular reference to semi-transparent PV cells using a-Si and perovskite as substrate, may contribute significantly to reduce energy demands in buildings by means of a twofold action. On one side the cells behave as solar control glasses, thus dramatically reducing solar gains during both heating and cooling season, with particular benefit in the second case. This benefit proved to be significant in all the cases (both office and residential building). Secondly, the cells produce electricity with different behaviors in relation to solar radiation. Perovskite cells efficiency varies linearly with solar radiation, while a-Si cells have a much more constant behavior, with efficiency dropping only at very low intensities. Consequently, despite the poorer performance under STC, a-Si cells performed better than perovskite cells. However, in terms of visual comfort perovskite cells offered a more balanced behavior, limiting both under-illumination and over-illumination, and allowing additional savings in terms of electricity for office lighting. In addition, the neutral coloration of perovskite cells offers an advantage that is hard to quantify using purely energetic parameters, but may certainly affect comfort conditions of the occupants. Further investigations would be required to take into account such effects, as well as to account for economic evaluation (as soon as more realistic data would be available) to assess the effective convenience of BIPV technologies.

Acknowledgments

This activity was partially funded by the Action Co-founded by Cohesion and Development Fund 2007-2013 – APQ Research Puglia Region "Regional programme supporting smart specialization and social and environmental sustainability – FutureInResearch".

References

[1] Jelle BP, Breivik C. (2012) The path to the building integrated photovoltaics of tomorrow. *Energy Procedia* (2012);20:78–87.
[2] Mercaldo LV, Addonizio ML, Noce M Della, Veneri PD, Scognamiglio A, Privato C. (2009) Thin film silicon photovoltaics: Architectural perspectives and technological issues. *Appl Energy* (2009);86:1836–44. doi:10.1016/j.apenergy.2008.11.034.
[3] Carlson DE, Wronski CR. (1976) Amorphous silicon solar cell; *Appl. Phys. Lett.* (1976); 28 671:1–4. doi:10.1063/1.88617.
[4] Martin A. Green, Keith Emery, Yoshihiro Hishikawa (2015) WW and EDD. Solar cell efficiency tables (Version 45). *Prog Photovolt Res Appl* 2015;23:1–9. doi:10.1002/pip.
[5] Saifullah M, Gwak J, Yun JH. (2016) Comprehensive review on material requirements, present status, and future prospects for building-integrated semitransparent photovoltaics (BISTPV). *J Mater Chem A* (2016);4:8512–40. doi:10.1039/C6TA01016D.
[6] Song Z, Phillips AB, Krantz PW, Khanal RR, Heben MJ. (2014) Spray pyrolysis of semi-transparent backwall superstrate CuIn(S,Se)2 solar cells. *IEEE 40th Photovolt Spec Conf PVSC 2014* (2014):1712–7. doi:10.1109/PVSC.2014.6925251.
[7] Tan H, Furlan A, Li W, Arapov K, Santbergen R, Wienk MM, et al. (2016) Highly Efficient Hybrid Polymer and Amorphous Silicon Multijunction Solar Cells with Effective Optical Management. *Adv Mater* (2016);28:2170–7. doi:10.1002/adma.201504483.
[8] Cannavale A, Eperon GE, Cossari P, Abate A, Snaith HJ, Gigli G. (2015) Perovskite photovoltachromic cells for building integration. *Energy Environ Sci* (2015);8:1578–84.
[9] Gaspera E Della, Peng Y, Hou Q, Spiccia L, Bach U, Jasieniak JJ, et al. (2015) Ultra-thin High efficiency semitransparent perovskite solar cells. *Nano Energy* (2015);13:249–57. doi:10.1016/j.nanoen.2015.02.028.
[10]Eperon GE, Burlakov VM, Goriely A, Snaith HJ. (2014) Neutral color semitransparent microstructured perovskite solar cells. *ACS Nano* (2014);8:591–8. doi:10.1021/nn4052309.
[11]Boyce P, Eklund N, Mangum S, Saalfield C, Tang L. (1995) Minimum acceptable transmittance of glazing. *Light Res Technol* (1995);27:145–52. doi:10.1177/14771535950270030201.
[12]Chae YT, Kim J, Park H, Shin B. (2014) Building energy performance evaluation of building integrated photovoltaic (BIPV) window with semi-transparent solar cells. *Appl Energy* (2014);129:217–27. doi:10.1016/j.apenergy.2014.04.106.
[13]Oliver M, Jackson T. (2001) Energy and economic evaluation of building-integrated photovoltaics *Energy* (2001);26:431–9.
[14]Favoino F, Fiorito F, Cannavale A, Ranzi G, Overend M. (2016) Optimal control and performance of photovoltachromic switchable glazing for building integration in temperate climates. *Appl Energy* (2016);178:943–61. doi:10.1016/j.apenergy.2016.06.107.
[15]Lim JW, Lee SH, Lee DJ, Lee YJ, Yun SJ. (2013) Performances of amorphous silicon and silicon germanium semi-transparent solar cells. Thin Solid Films (2013);547:212–5. doi:10.1016/j.tsf.2013.03.038.
[16]Hörantner MT, Nayak PK, Mukhopadhyay S, Wojciechowski K, Beck C, McMeekin D, et al. (2016) Shunt-Blocking Layers for Semitransparent Perovskite Solar Cells. *Adv Mater Interfaces* (2016) 1500837, doi:10.1002/admi.201500837.
[17]Cannavale A, Hörantner M, Eperon GE, Snaith HJ, Fiorito F, Ayr U, Martellotta F. (2017) Building integration of semitransparent perovskite-based solar cells: Energy performance and visual comfort assessment. *Appl Energy* (2017);194:94–107. doi:10.1016/j.apenergy.2017.03.011.
[18]Randall JF, Jacot J, (2003) Is AM1.5 applicable in practice? Modelling eight photovoltaic materials with respect to light intensity and two spectra, *Renewable Energy* (2003) 28: 1851–1864
[19]United States Dept. Of Energy (2016), *EnergyPlus version 8.6 documentation, Engineering Reference*.
[20]ASHRAE (2012). International Weather for Energy Calculations (IWEC Weather Files) Version 2.0. Atlanta: ASHRAE.
[21]Mardaljevic J, Andersen M, Roy N, Christoffersen J (2012), Day lighting metrics: is there a relation between useful daylight illuminance and daylight glare probability? Proceedings of the building simulation and optimization conference (BSO12), Loughborough, UK (2012).